CMOS Charged Particle Spectrometers

G. A. Soli, H. B. Garrett, and E. R. Fossum

Center for Space Microelectronics Technology
Jet Propulsion Laboratory
California Institute of Technology
Pasadena, CA 91109

Abstract

Integrated circuits, manufactured in CMOS technology, have been developed as diffusion-based charged particle spectrometers for space applications. Current designs are single-chip spectrometers capable of uniquely identifying and counting electrons and heavy ions. A four-chip spectrometer designed to count protons and heavy ions was flown on the Clementine spacecraft. The spectrometer proton data is compared to GOES-6 proton data for the 21 February 1994 solar proton event.

I. INTRODUCTION

Flight data from a four-chip CMOS spectrometer designed to count protons for the Clementine spacecraft is presented. These chips are configured as SRAMs for integral spectroscopy. The spectrometer proton data is compared to GOES-6 proton data for the 21 February 1994 solar proton event. The Active Pixel Sensor (APS) chips are differential spectrometers. APS noise floor measurements are shown to extend CMOS charged particle spectrometer methods into the electron region. Space Technology Research Vehicle-2 (STRV-2) APS CMOS proton and electron spectrometer design methods are presented. CMOS charged particle spectrometers represent a low cost method of collecting trapped charged particle data for replacing the AE8 electron and AP8 proton models, the international radiation design standards used in earth orbiting spacecraft design.

II. CMOS SRAM SPECTROMETER DESIGN

A schematic diagram of the SRAM cell is shown in Figure 1. The pulsed current source is used to model a particle strike on drain Dn2 when calculating the critical charge required to upset a cell with SPICE [1]. Charge is digitized within each cell making the SRAM design insensitive to radiation induced dark current [2]. This cell differs from that of a standard six-transistor SRAM cell in three ways: (1) the source of the p-MOSFET, Mp2, is connected to an adjustable offset voltage, V_O, instead of V_{DD} to provide a control of the cells critical charge; (2) the drain area of n-MOSFET Mn2, Dn2, has been enlarged by a factor of four over minimum to enhance upset rates, thus reducing measurement time; and (3) the cell is imbalanced by widening Mn2 over minimum to enhance its sensitivity to charged particles versus V_O.

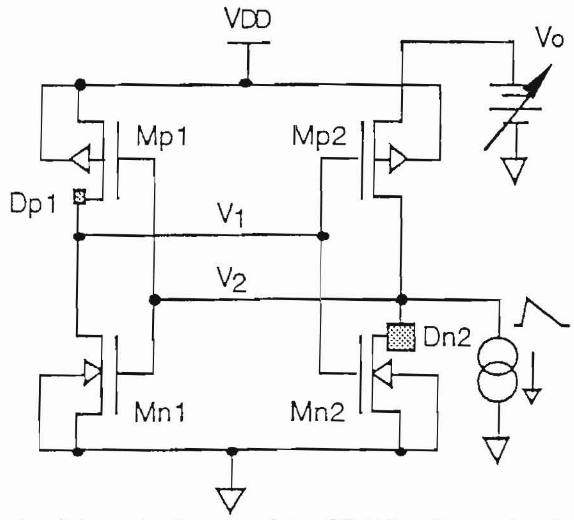

Figure 1. Schematic diagram of the SRAM cell showing the placement of V_O and the bloated n-drain, Dn2

In operation all the memory cells are written into a "sensitive" state where Mn2 is turned OFF and Mp2 is turned ON, connecting V_O to the bloated drain, Dn2. V_O is then lowered from V_{DD} = 5 V allowing the SRAM to accumulate cell upsets at a given V_O value. Thereafter V_O is returned to V_{DD} and the cells read to determine the number of cell upsets.

III. CMOS APS SPECTROMETER DESIGN

Current CMOS chip spectrometer designs are Active Pixel Sensor (APS) chips that are also being developed by NASA as, light weight, low power, optical imagers [3,4,5]. APS spectrometers are being utilized on the STRV-2 to count trapped protons and electrons and to demonstrate electron counting. The STRV-2 APS and the Clementine SRAM spectrometers are both fabricated in 1.2 µm n-well technology through MOS Implementation System (MOSIS).

The CMOS APS, along with readout circuits, is shown schematically in Figure 2 [4]. The pixel unit cell consists of a photodiode (PD), a source-follower input transistor, a row-selection transistor and a row-reset transistor. At the bottom of each column of pixels, there is a load transistor VLP and two output branches to store the reset and signal levels. Each branch consists of a sample and hold capacitor (CS or CR) with a sampling switch (SHS or SHR) and a second source-follower with a column-selection switch (COL).

0018-9499/96$05.00

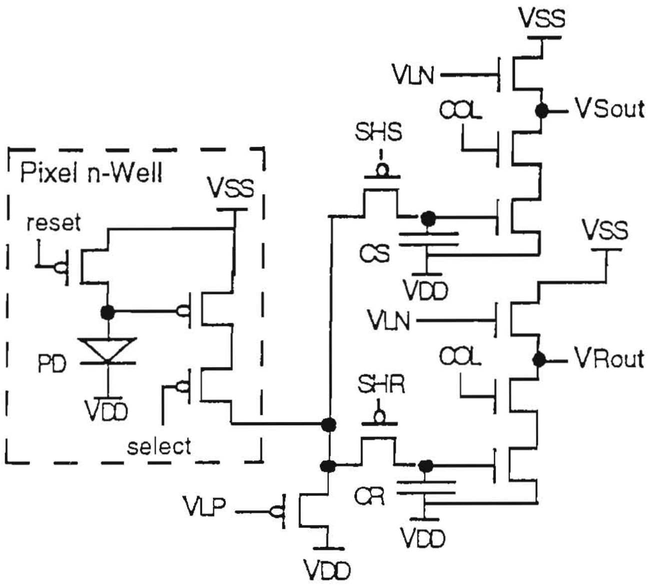

Figure 2. APS CMOS photodiode pixel circuit schematic showing pixel, with row reset and row select, and column sample and hold capacitors.

The reset and signal levels are read out differentially, suppressing 1/f noise and fixed pattern noise (not kTC noise) from the pixel. If the signal levels are read out twice, once before integration and once after integration, kTC noise is also suppressed [6]. These readout circuits are common to an entire column of pixels. The load transistors of the second set of source followers (VLN) are common to the entire array. In operation a row is selected and the signal level V_3 is stored on CS. The row is then reset and reset level V_4 is stored on CR. Each column is then readout through a differential amplifier giving $(V_3\text{-}V_4)$. This voltage difference can be histogrammed and a new row selected or stored in memory for kTC noise suppression. For kTC noise suppression the row must be readout twice each time it is selected [6]. The row is reset again, after the first column read and reset level V_1 is stored on CR. The row reset is then turned off and signal level V_2 is stored on CS. Each column is then readout for the second time giving $(V_2\text{-}V_1)$. For frame number n, pixel kTC noise is suppressed by the following equation:

$$V^* = (V_3\text{-}V_4)_{n+1} - (V_2\text{-}V_1)_n \qquad (1)$$

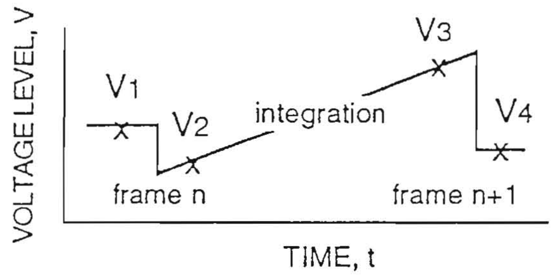

Figure 3. Photodiode type APS kTC noise supperession voltage measurement diagram showing reset levels V_1 and V_4, and signal levels V_2 and V_3.

The voltage V* is then histogrammed and the next row is selected. Figure 3 shows these voltage levels as a function of time. This operation does not suppress CR and CS kTC noise. For typical APS on-chip capacitor designs the CR and CS kTC noise is about 0.3, in sigma, times the pixel kTC noise without pixel kTC noise suppression. Test structures designed to separate noise sources as a function of total radiation dose are currently being tested.

IV. SRAM SPECTROMETER CALIBRATION

Selected SRAMs from the Clementine flight fabrication run were calibrated with protons. In effect, protons were used to measure a Si equivalent dead layer or over layer thickness and a Si charge collection layer thickness for the Clementine SRAM. The APS values are estimated for use in chip design. Figure 4 shows the Clementine SRAM and STRV-2 APS layer thicknesses and the labeling convention used in modeling calibration data, where E2 is the particle energy above the chip, $\Delta E3 = E2 - E3$ is the energy lost in the over layer, and $\Delta E4 = E3 - E4$ is the energy deposited in the charge collection layer.

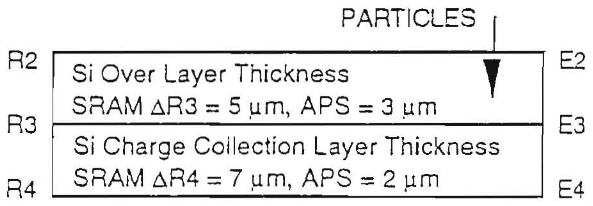

Figure 4. 1.2 μm technology labeling convention and layer thicknesses used in modeling calibrations.

Proton energy as a function of range is computed using the fit equation shown in Figure 5. This equation is derived from a fit to the TRIM [7] computer code. The error bars indicate longitudinal range straggling.

The Clementine proton spectrometer design, SRAM cell, is an integral spectrometer [1]. All particles depositing more than the threshold energy are counted. Representative chips from the flight fabrication run were calibrated using the Caltech Tandem Van de Graaff proton accelerator. Calibration data was taken at normal incidence with 0.75, 1.0, and 2.0 MeV protons. The mean value threshold energies, where half the protons hitting a sensitive node, Dn2, are counted. These mean values are plotted in Figure 6. The proton calibration data points are the mean values of the delta offset voltage, ΔV_p, where one-half the protons hitting a cell sensitive volume cause the cell to flip. The delta offset voltage is the operating offset voltage minus the spontaneous flip voltage. The spontaneous flip voltage is the offset voltage value where one-half the SRAM cells have spontaneously flipped. The proton data calibrated the 1.2 μm technology SRAM at an upset capacitance, $C_u/K = 2.667$ (MeV/V), where $K = 44.2$ (fC/MeV) for proton produced ionization per unit energy loss in silicon.

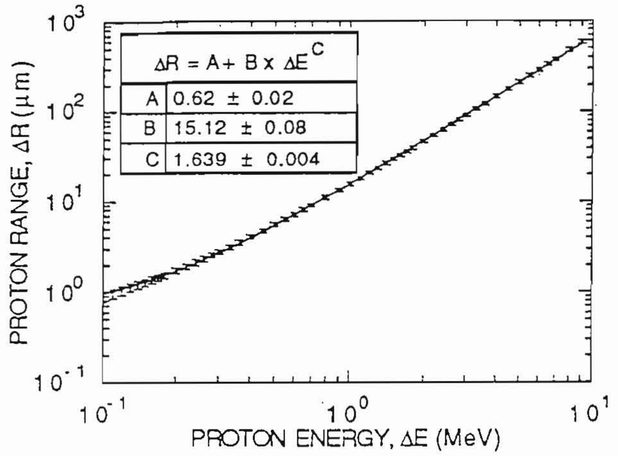

Figure 5. Fit to TRIM generated proton range as a function of energy in silicon. The error bars indicate longitudinal straggling.

The measured energy, ΔE4 shown in Figure 6, is given by, $\Delta E4 = (C_u/K) \times (\Delta V_p)$. The 1 MeV energy window bracketing the injection peak, also shown in Figure 6, is the measure of the SRAM response to protons in the space environment. The response curves are computed by solving the TRIM fit equation shown in Figure 5 for energy ΔE as a function of range ΔR. The maximum cord lengths are ΔR3 = 6.78 μm and ΔR4 = 11.46 μm.

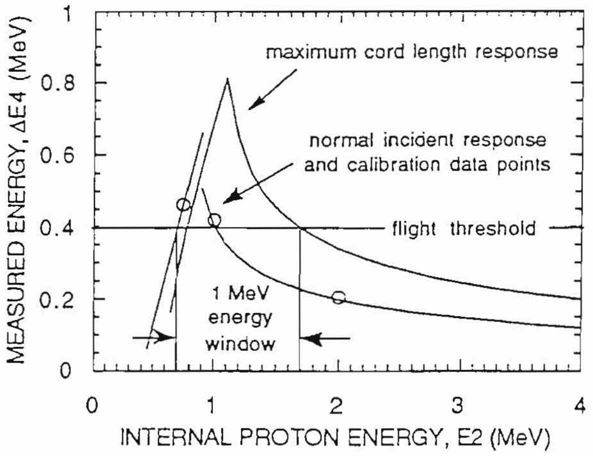

Figure 6. Clementine proton injection peak calibration curves showing the flight energy threshold and the 1 MeV wide energy window above the flight threshold.

V. CLEMENTINE FLIGHT DATA

On Clementine the proton energy spectrum was measured by counting protons in the 1 MeV wide energy window with four chips each behind a different shielding thickness [2]. The shields consisted of 10 mil kovar chip lids. The 0-lid chip had a hole drilled through its lid over the chip and the hole was covered with a 1 mil aluminium equivalent aluminized kapton dust cover. The chip-lid shields reduced the external environment proton energy, E1, and flux. The flux reduction is given by the environment fractions, f_e. The environment fractions were computed with the Novice code from a 2π-sr omnidirectional fluence of 1.96E9 (protons/cm^2-MeV) at all energies (0.1 to 100 MeV) outside the shields. The proton fluence is reduced by the amount f_e inside the shields. The resulting environment fractions as a function of proton energy inside the shields is shown in Figure 7. The 1 MeV wide energy window is also shown.

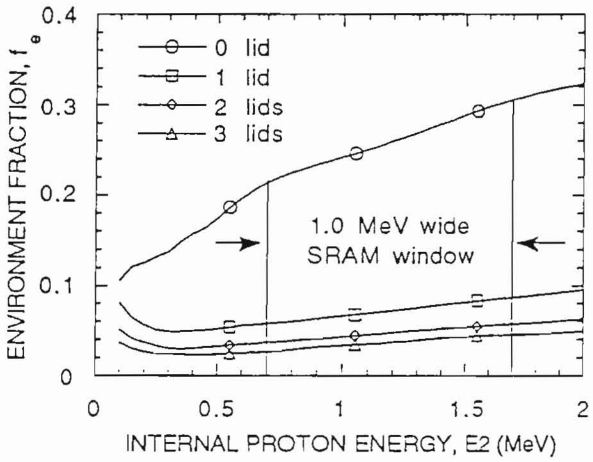

Figure 7. Environmental fraction as a function of proton energy inside lid shields. The 1 MeV wide proton sensitive window is shown.

Table 1 lists the external environment energy windows, Emin to Emax, measured in the 1 MeV wide energy window shown in Figures 6 and 7, as a function of shield thickness. The mean value of the environment fractions inside the energy window are also listed in table 1.

Table 1
External environment energy windows and internal environment fractions, f_e, as a function of shielding.

kovar shields (ch# - mils)	Emin (MeV)	Emax (MeV)	f_e mean value (0.7-1.7 MeV)
P1 - 0	2.16	3.16	0.261±0.031
P2 - 10	11.81	12.81	0.072±0.009
P3 - 20	16.96	17.96	0.047±0.007
P4 - 30	21.04	22.04	0.037±0.006

The Clementine spectrometer is sensitized to protons for 100 seconds, every other 100 second period, for one hour, giving an on time fraction, f_{on}, of 0.5. During the other 100 second period the threshold is lifted above the computed injection peak value, shown in Figure 6 for protons, to measure proton induced nuclear reactions. The energy window width, ΔE measured with protons, also shown in Figure 6, is 1 MeV. The instrument is designed with a 2π-sr field of view, Ω. The pixel sensitive area has an as drawn cross section, σ, of 42.12 μm^2. Each pixel can only count one proton in each 100 second proton sensitive period and there are 18 sensitive periods each hour. There are 4096 pixels, N_T, on each chip and N is the measured number of counts per hour in each chip. The spectrometer measured hourly fluence, F, in units of (protons/cm^2-sr-MeV-hr) outside the shields is given by:

$$F = \frac{18}{\sigma\, \Omega\, \Delta E\, f_e\, f_{on}} \ln\left(\frac{N_T}{N_T - N/18}\right) \qquad (2)$$

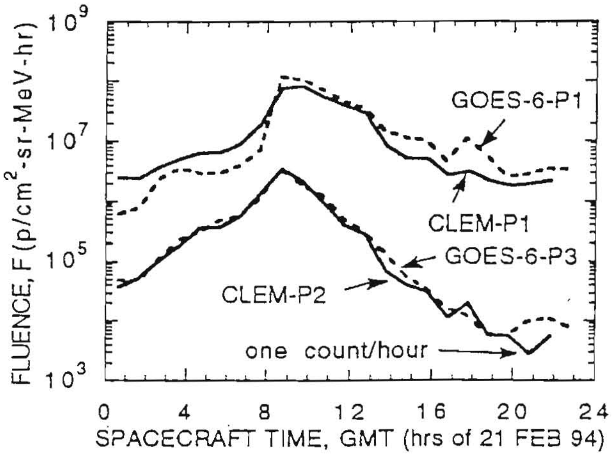

Figure 8. Comparison of Clementine data to GOES-6 data during the 21 Feb. 94 solar proton event. The proton spectrometer sensitivity of one count per hour is shown.

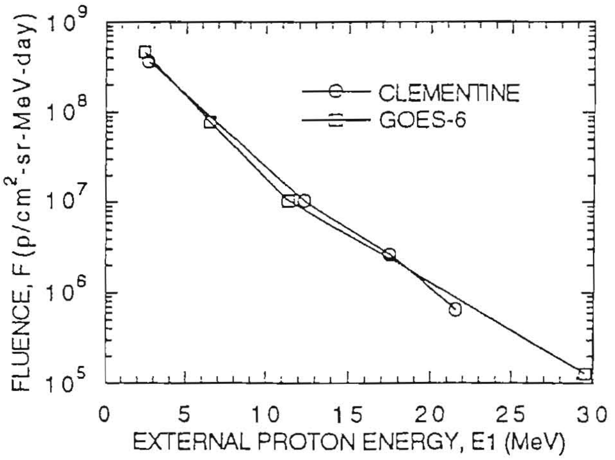

Figure 9. Clementine spacecraft and GOES-6 external environment proton energy (E1) spectra on 21 Feb. 94.

The Clementine spectrometer hourly fluences, F from Equation 2, and GOES-6 hourly fluencies are plotted in Figure 8. The GOES-6 external-environment proton-energy windows, Emin and Emax, are, P1 = 0.6 to 4.2 MeV, P2 = 4.2 to 8.7 MeV, P3 = 8.7 to 14 MeV, and P4 = 15 to 44 MeV. The Clementine and GOES-6 energy spectra for the total measured fluence on 21 Feb. 94 are shown in Figure 9. The data point energies, E1, are taken at the center of the energy windows, (Emin + Emax)/2, listed in Table 1 for the Clementine instrument and above for the GOES-6 instrument.

VI. APS SPECTROMETER CALIBRATION

The partial charge collection from peripheral hits would contaminate electron data. Both the Clementine SRAM and the standard APS photodiode collect partial charge from peripheral hits outside their sensitive nodes. The response to alpha particles is shown in Figure 10. The partial charge collection from hits outside the sensitive nodes makes these designs unusable for electron counting. For this reason the STRV-2 APS pixel is designed to suppress peripheral hit charge collection by blocking charge diffusion paths to the sensitive node. This is partially accomplished by placing the pixels in a n-well. The well geometry changes the charge collection thickness, as shown in Figure 4. All poly and metal layers are removed from above the sensitive node reducing the over layer thickness. The new thicknesses are estimated in Figure 4 and used to compute the expected STRV-2 APS response shown in Figure 11. The SRAM is an integral spectrometer and the count curve, shown in Figure 10, is the derivative of the measured curve. The device voltage for the SRAM is the offset voltage value for a given count measurement. The APS is a differential spectrometer and the device voltage is the output voltage histogrammed in a multichannel analyzer.

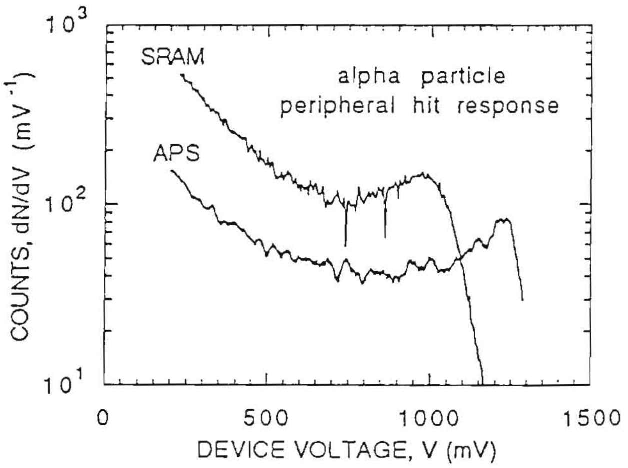

Figure 10. SRAM and APS alpha particle response showing partial charge collection from peripheral hits outside the sensitive nodes. The SRAM data is the derivative of the measured counts.

Particle identification regions are shown in Figure 11. The measured energy in these regions is unique for each particle type. The APS design is a differential spectrometer where the pulse height associated with each measured energy is histogrammed into a differential energy spectrum. This allows the APS to operate with unity on-time fraction, f_{on}. A 60° cutoff angle is used to compute the maximum cord length response in Figure 11. Reducing this angle would decrease the energy window widths.

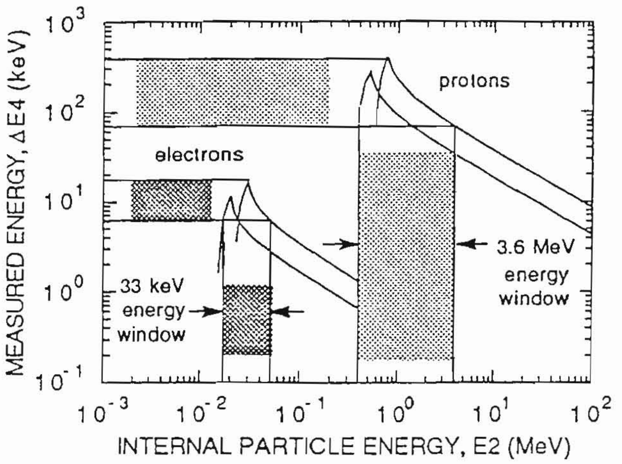

Figure 11. APS n-well pixel, normal incident and 60° maximum cord length, measured energy regions that are unique to each particle type as a function of the particle E2 energy windows.

The APS design extends CMOS spectrometers into the electron region shown in Figure 11. The standard photodiode APS design room temperature noise floor, without kTC noise suppression, is measured with 5.9 keV X-rays and this is compared to the SRAM spontaneous flip curve derivative in Figure 12. The APS X-ray spectrum was taken after a 1 krad silicon total Co-60 dose. The APS noise is about one quarter fixed pattern and three quarters in pixel, one half kTC and one half all other sources including radiation induced dark current shot noise. The SRAM noise is fixed pattern dominated and has no dark current shot noise component.

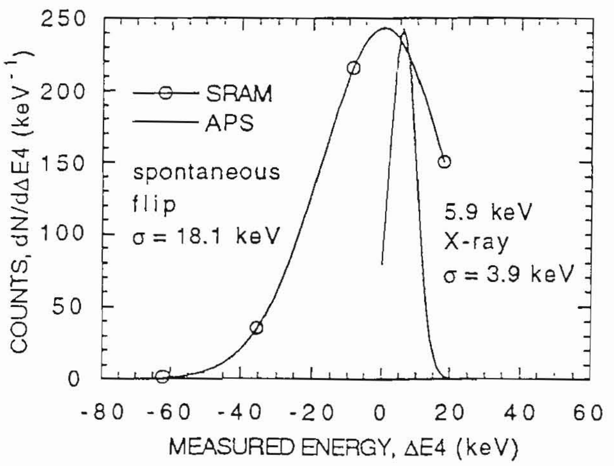

Figure 12. Post radiation APS calibration at room temperature showing 55-Fe X-ray peak fit and the SRAM spontaneous flip curve derivative.

VII. Conclusions

The CMOS charged particle spectrometer injection peak energy window and shield energy filter approach to measuring charged particle energy spectra in space has been proven as a low mass and low power method on the Clementine flight experiment. The differential spectrometer APS design approach allows unity on time fraction operation. The APS noise floor extends CMOS charged particle spectrometer methods into the electron region. The STRV-2 flight will verify the APS CMOS charged particle spectrometer as a low cost method of collecting trapped charged particle data for replacing AE8 electron and AP8 proton models, the international radiation standards used in earth orbiting spacecraft design.

VIII. Acknowledgments

The research described was performed by the Center for Space Microelectronics Technology, Jet Propulsion Laboratory, California Institute of Technology, and was sponsored by the Ballistic Missile Defense Organization, Innovative Science and Technology Office (BMDO/IST). Author Henry Garrett would like to thank Col. Peter Rustan, Col. Peter Worden, and Dr. Dwight Duston for their encouragement and support during his tour of duty with BMDO/IST. The authors are indebted to Martin Buehler, Brent Blaes, Peter Jones, Martin Ratliff, Ken Hicks, Kevin Watson, Ken McCarty, and Tom Sorensen; the Clementine experiment team members. And to USC/ISI/MOSIS project for the fabrication of the test structures used in the Clementine experiment. And to Alan Rice, at the Caltech Tandem Van de Graaff, for his assistance in performing the proton calibration experiments.

IX. References

[1] G. A. Soli, B. R. Blaes, and M. G. Buehler; "Proton-Sensitive Custom SRAM Detector"; IEEE Trans. Nuclear Science, Vol. 39, pp. 1374-1378, Oct. 1992.

[2] G. Soli, B. Blaes, M. Buehler, P. Jones, J. Ratliff, and H. Garrett; "Clementine Dosimetry" AIAA "Journal of Spacecraft and Rockets", Vol. 32, No. 6, Nov.-Dec. 1995.

[3] E. R. Fossum; "Low Power Camera-on-a-Chip Using CMOS Active Pixel Sensor Technology" 1995 Symposium on Low Power Electronics. Oct. 9-10, 1995 San Jose, CA.

[4] R. H. Nixon, S. E. Kemeny, C. O. Staller, and E. R. Fossum; "128x128 CMOS Photodiode-Type Active Pixel Sensor with On-Chip Timing, Control and Signal Chain Electronics"; SPIE Proceedings, Vol. 2415, paper 34, (1995)

[5] R. H. Nixion, S. E. Kemeny, C. O. Staller and E. R. Fossum; '256x256 CMOS Active Pixel Sensor Camera-on-a-Chip" to be presented at 1996 IEEE International Solid-State Circuits Conference, Feb. 8-10, 1996

[6] L. Ramirez, R. Hickok, B. Pain, and C. Staller; "Implementation of a Noise Reduction Curcuit for Spacecraft IR Spectrometers," in Infrared Readout Electronics. Proc. SPIE, vol. 1684, pp. 247-256 (1992)

[7] Ziegler, J. F., Biersack, J. P. and Littmark, U.; The Stopping and Range of Ions in Solids. Pergamon Press (New York, NY, 1985).